MIT Open Access Articles

A deep learning approach to classify atherosclerosis using intracoronary optical coherence tomography

PROCEEDINGS OF SPIE

A deep learning approach to classify atherosclerosis using intracoronary optical coherence tomography

Lambros S. Athanasiou, Max L. Olender, José M. de la Torre Hernandez, Eyal Ben-Assa, Elazer R. Edelman

SPIE.

A deep learning approach to classify atherosclerosis using intracoronary optical coherence tomography

Lambros S. Athanasiou[*a,b], Max L. Olender[a,c], José M. de la Torre Hernandez[d], Eyal Ben-Assa[e,f], Elazer R. Edelman[a,b]

[a]Institute for Medical Engineering and Science, Massachusetts Institute of Technology, Cambridge, MA, United States; [b]Cardiovascular Division, Brigham and Women's Hospital, Harvard Medical School, Boston, MA, United States; [c]Department of Mechanical Engineering, Massachusetts Institute of Technology, Cambridge, MA, United States; [d]Hospital Universitario Marques de Valdecilla, Unidad de Cardiologia Intervencionista, Servicio de Cardiologia, Santander, Spain; [e]Massachusetts General Hospital, Harvard Medical School, Cardiology Division, Department of Medicine, Boston, MA United States; [f]Tel Aviv Sourasky Medical Center, Sackler Faculty of Medicine, Cardiology Division, Tel Aviv, Israel

ABSTRACT

Optical coherence tomography (OCT) is a fiber-based intravascular imaging modality that produces high-resolution tomographic images of artery lumen and vessel wall morphology. Manual analysis of the diseased arterial wall is time consuming and sensitive to inter-observer variability; therefore, machine-learning methods have been developed to automatically detect and classify mural composition of atherosclerotic vessels. However, none of the tissue classification methods include in their analysis the outer border of the OCT vessel, they consider the whole arterial wall as pathological, and they do not consider in their analysis the OCT imaging limitations, e.g. shadowed areas. The aim of this study is to present a deep learning method that subdivides the whole arterial wall into six different classes: calcium, lipid tissue, fibrous tissue, mixed tissue, non-pathological tissue or media, and no visible tissue. The method steps include defining wall area (WAR) using previously developed lumen and outer border detection methods, and automatic characterization of the WAR using a convolutional neural network (CNN) algorithm. To validate this approach, 700 images of diseased coronary arteries from 28 patients were manually annotated by two medical experts, while the non-pathological wall and media was automatically detected based on the Euclidian distance of the lumen to the outer border of the WAR. Using the proposed method, an overall classification accuracy 96% is reported, indicating great promise for clinical translation.

Keywords: Optical coherence tomography, Deep learning, Atherosclerosis, Convolutional neural network

1. INTRODUCTION

Intravascular optical coherence tomography (OCT)[1,2] is a catheter-based imaging modality developed over recent decades that has become popular in interventional cardiology. OCT has much higher resolution than other intravascular imaging modalities, like intravascular ultrasound (IVUS): 12-18 microns axially and a lateral resolution of 20-90 microns[3]. OCT calculates the proportion of the light backscattered and absorbed by the vessel tissue and reconstructs two-dimensional (2D) images which represent the cross sections of the imaged vessel.

OCT can provide accurate measurements of a vessel's lumen, assess wall morphology, and allow detection of four different tissue types[4]: calcium (CA), lipid tissue (LT), fibrous tissue (FT), and mixed tissue (MT). Moreover, it enables the detection of features that are associated with plaque vulnerability, including the measurement of fibrous cap thickness, which cannot be accurately evaluated by IVUS or by any other intravascular imaging technique[5]. However, the technology has a serious drawback, the limited tissue penetration (maximum depth: 1.5-2.0 mm)[4], which may not allow visualization and assessment of the entire plaque and the media-adventitia border.

The aforementioned limitation of OCT led to the implementation of automated analysis methodologies that detected only the lumen border of the vessel[6–9], or the lumen border and estimated the plaque area of the vessel[10,11]. Since manual plaque

---

[*] lambros@mit.edu; lmathanas@gmail.com; phone +1 617 715 4569.

characterization is time consuming and relies on well-trained readers, several studies attempted to automatically detect the various plaque components using OCT images[12]. Xu et al.[13] correlated the backscattering and attenuation coefficients with CA, LT, and FT, while, in a similar attempt, van Soest et al.[14] correlated the attenuation coefficients with healthy vessel wall, intimal thickening, lipid pool, and macrophage infiltration. However, they both failed to define any clear threshold values between the different tissue types. Going one step further and using machine learning, Athanasiou et al.[10] presented a fully-automated OCT plaque characterization method which classified plaque as CA, LT, FT, or MT, with 83% accuracy. More recently, deep learning approaches using convolutional neural networks (CNNs)[15–18] were presented, achieving an overall accuracy of up to 91.7%[18].

Although, CNN-based methods outperformed machine learning methods, they all failed to characterize the whole arterial wall, resulting in methods which cannot compete with widely-used virtual histology IVUS (VH-IVUS)[19], limiting the imaging detail superiority benefits of OCT when compared to IVUS. The primary drawbacks hampering automated OCT plaque characterization are the lack of large amounts of annotated images and the non-realistic tissue (area of interest) segmentation caused by the difficulty of automatically detecting the outer border. The proposed approach leverages our recently developed lumen[8] and outer border detection[20] algorithms to introduce an automated method which characterizes the whole arterial wall. We present a novel and accurate method for detecting and characterizing, for the first time, the whole arterial tissue in a way similar to VH-IVUS.

The innovative aspects of proposed tissue characterization method are:

1. use of CNNs with a large amount of annotated data to detect atherosclerosis;

2. detection of normal tissue and shadowed areas within the OCT images; and

3. detection and classification of the whole arterial wall using OCT images in a similar way as VH-IVUS performs its analysis, enabling the wide use of OCT in atherosclerotic tissue detection.

2. MATERIALS AND METHODS

The proposed method (Figure 1) comprises the following three steps:

1. wall area (WAR) detection using previously developed lumen and outer border detection methods;

2. definition of the non-pathologic intima-media area; and

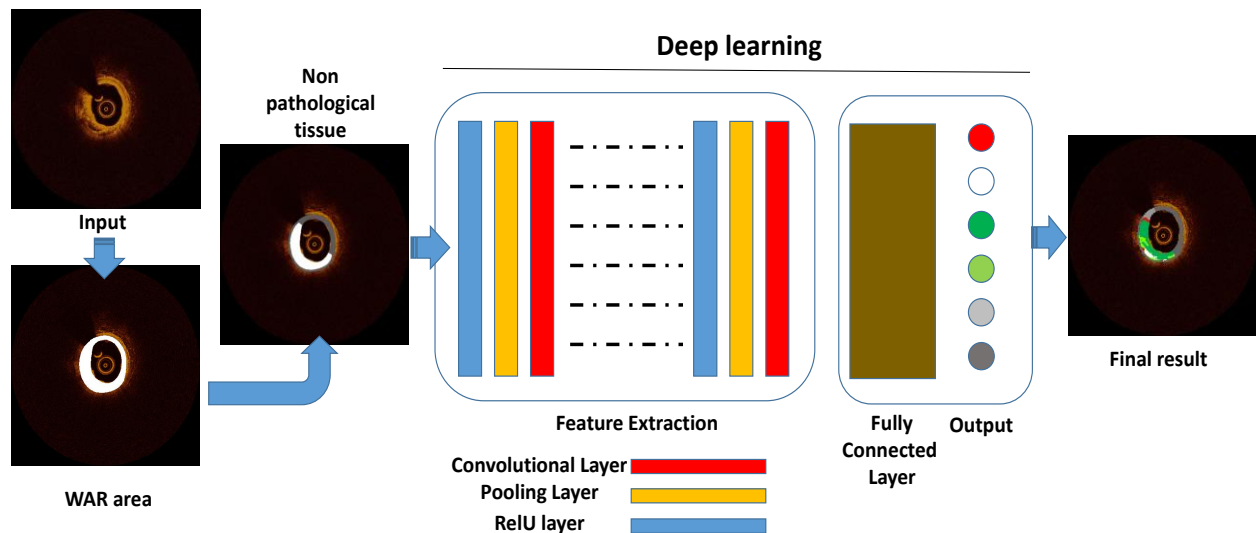3. automatic characterization of the WAR using a CNN algorithm.

Figure 1: Schematic presentation of the proposed methodology.

2.1 Wall area detection

WAR is defined as the area between the lumen and outer border (Figure 2), i.e. the media-adventitia transition. The lumen detection method uses as input 2D cross-sectional OCT images, produces longitudinal cross-sectional images (sagittal cuts) which represent more accurately the sequential area of the OCT pullback, detects the lumen by applying bilateral filtering and a K-means algorithm, and translates the detected lumen to the 2D OCT images[8]. The outer border detection method detects the outer vessel border within segments of the OCT pullback that are visible and then, by using a unique 3D surface-fitting method, fills the non-visible parts[20].

2.2 Non-pathologic intima-media area detection

Once the lumen and media-adventitia borders are detected, the non-pathological tissue and media layer (M) of the WAR are defined. The concept is based on the VH-IVUS histology method where the normal vessel wall has intimal thickening of <300μm[4,19]. To measure the distance of the two borders, we calculate for each pixel of the WAR, $p \in WAR$, the combined distance of the pixel from the lumen and media-adventitia borders:

$$D_{L-MA} = D_1 + D_2,$$ (1)

and the distance of the pixel from the media-adventitia border: $D1$.

Here, D_1 is the Euclidean distance of the pixel p from the media-adventitia border and D_2 is the Euclidean distance of the pixel p from the lumen border; if $D1 < 100$μm or $D_{L-MA} <300$μm the pixel belong to M. A schematic presentation of the two distances is shown in Figure 2.
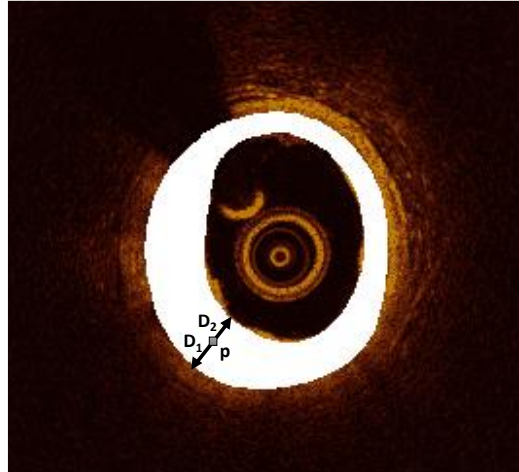

Figure 2: Schematic presentation of the two Euclidean distances calculated for defining the non-pathologic intima-media area (M) within the WAR (white).

2.3 CNN-based classification

After detecting the pixels that belong to the non-pathological tissue and media (M) area, the remaining WAR pixels are automatically classified into one of five categories including four plaque types: calcium (C), lipid tissue (LT), fibrous tissue (FT), or mixed tissue (MT), and no visible tissue (catheter artifact; N), using a CNN network.

2.3.1 CNN algorithm

CNNs belong to the family of deep learning networks[21], and are commonly used to analyze and classify images. They consist of an input and an output layer with multiple hidden layers between them. The hidden layers consist of several convolutional layers which automatically extract the complex features of the images.

A CNN is represented by a non-linear function:

$$p_i = P(I; \theta)$$ (2)

which maps an image $I \in \mathbb{R}^{H \times H}$ having $H \times H$ size, to a vector $p_i = (p_1, p_2, ... p_c)^T$, where $p_i \in [0,1]$ and denotes the probability of the image I to belong to one of c classes: $i = 1 ... c$. $\theta = \{\theta_1, \theta_2, ... \theta_K\}$ are the number of K parameters used to map the input image I to the vector p_i.

The training of the CNN can be considered as a non-linear optimization problem:

$$\hat{\theta} = \arg_\theta \min L_{\{I^{(1)}, I^{(2)}, \ldots, I^{(N)}\}}(\theta). \tag{3}$$

Here, N is the number of images used to train the CNN, and

$$L_{\{I^{(1)}, I^{(2)}, \ldots, I^{(N)}\}}(\theta) = -\frac{1}{N} \sum_{j=1}^{N} w_j \, yC^{(i)T} logP(I^{(i)}; \theta) \tag{4}$$

is the cross-entropy loss (log loss) measuring the classification performance (having values between 0 and 1) for the $C^{(i)T}$ labeled vector of the c classes and w weights:

$$w_i = \frac{\frac{1}{M_i}}{\Sigma_{i=1}^{c} \frac{1}{M_i}}, \tag{5}$$

for the M training data.

To minimize the training time of the CNN, the Stochastic Gradient Descent (SGD) iterative method can be used. SGD approximates the dataset with a batch of random samples, using the stochastic gradient computed from the batch to update the model with each iteration[22]. SGD might oscillate along the path of steepest descent (gradient descent) towards the optimum, instead of along the path toward the optimal, since the gradient always points towards the opposite side of this optimum from the current position. A solution to that problem is adding a momentum term to the parameter update to reduce oscillation:

$$\theta_{\lambda+1} = \theta_\lambda - \alpha\nabla L(\theta_\lambda) + \gamma(\theta_\ell - \theta_{\lambda-1}), \tag{6}$$

where λ is the iteration number, $\alpha > 0$ is the learning rate, and the momentum term γ determines the contribution of the previous gradient step to the current iteration.

The SGD algorithm uses a subset of the training set called a mini-batch, evaluates the gradient, and then updates the parameters. Each evaluation is an iteration, and at each iteration the loss function is minimized further. The full pass of the training process over the whole training set using mini-batches forms an epoch.

2.3.2 CNN architecture

To classify the pixels of the WAR, we used a sequence of convolutions. To achieve the best classification results, different patch sizes, numbers of input patch convolution sequences, filters, and filter sizes were tested. The best results were acquires when having 45 layers in our network (Figure 3).

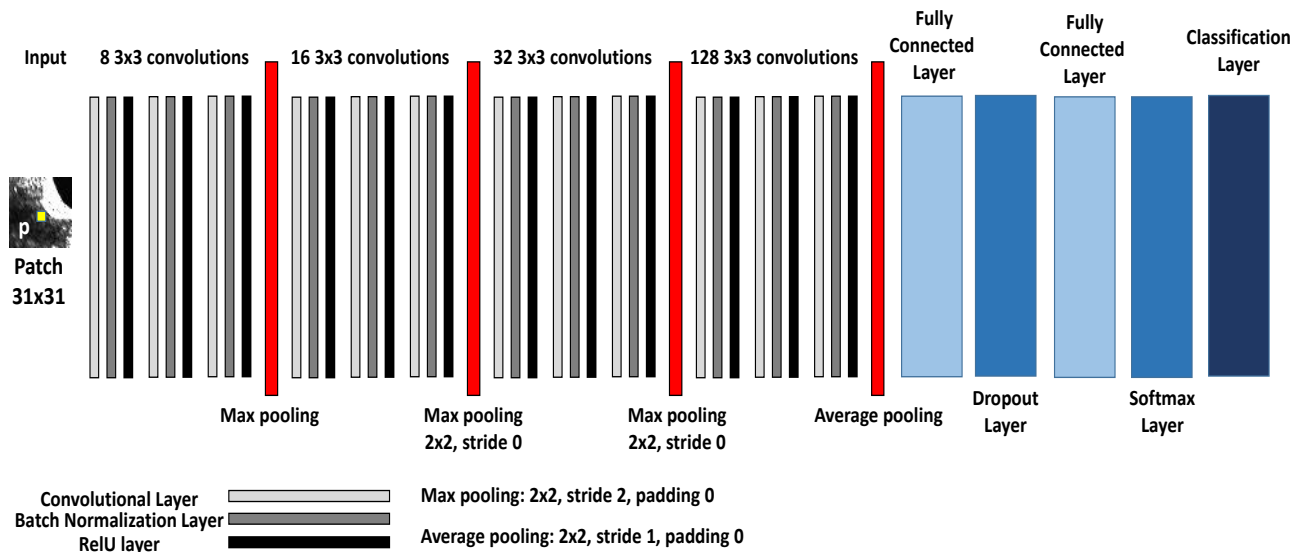
Figure 3: Architecture of the CNN used to classify the WAR pixels.

3. DATASET

Twenty-eight (28) patients who underwent OCT examinations gave their informed consent for the study, and the study was approved by the Ethics Committee of the institution. Medical experts used the optical frequency domain imaging system FD-OCT C7XR system and the DragonFly catheter (St. Jude Medical, Lightlab Imaging Inc., Westford, MA, USA), which offers a maximum frame rate of 100 frames per second, 500 lines per frame, a scan diameter of 10 mm, and axial resolution of 15 μm, to image 28 coronary vessels. All images were digitally stored in raw format for off-line analysis, and all imaging data sets were anonymized and transferred to our lab for further analysis.

4. RESULTS

3.1 Wall area detection

Two medical experts examined the OCT frames in the twenty two patients and selected 700 images which corresponded to diseased coronary segments. Afterwards, they marked independently the contours of the lumen border, the intima-media border, and regions of calcium (C), lipid tissue (LT), fibrous tissue (FT), mixed (C+ LT) plaque (MP), and the area of the catheter shadow (no visible tissue; N); any disagreements in their annotations were resolved by consensus. The areas detected by the algorithm and annotated by the experts were calculated and compared (Figure 4).
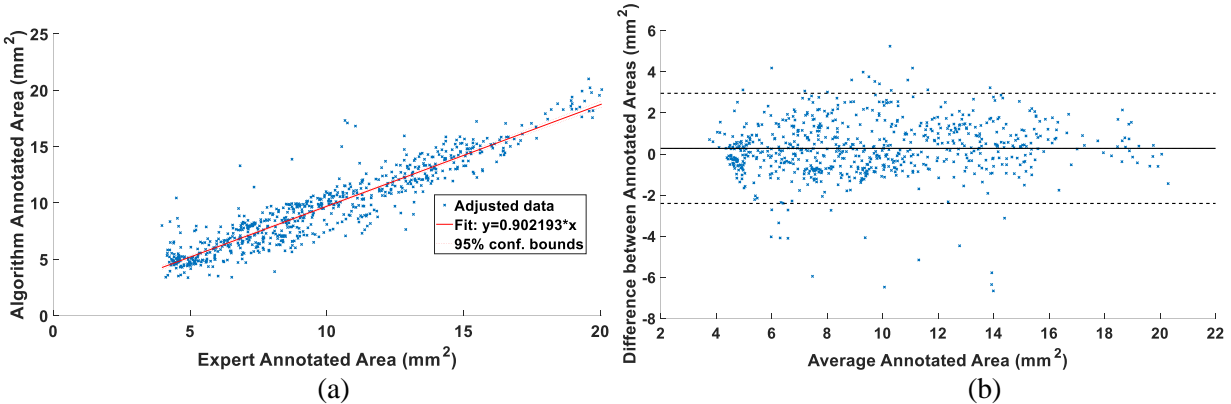

Figure 4: (a) Regression analysis plot between the WAR detected by our method and annotated by the experts and, (b) Bland and Altman analysis plot for the WAR detected by our method and annotated by the experts.

3.2 Plaque characterization

The medical experts completely annotated 300 different plaque regions for 22 of the patients, from which 32 K patches were randomly selected for each class and augmented (each patch rotated 90° and 180°), resulting in 480 K patches (96 K for each of the five classes). The patches were used to train (450 K) and validate (30 K) the CNN parameters. The CNN algorithm reached a validation accuracy of 94.00% (Figure 5).

One expert annotated 50 areas in the remaining 6 patients as C (9450 patches), LT (174448 patches), FT (216336 patches), MT (35301 patches), or N (408243 patches) regions to test the classification accuracy of the proposed method. The CNN network was trained and validated using the MATLAB Deep Learning Toolbox and a NVIDIA Titan Xp GPU (PG611) with 12 GB RAM. The overall accuracy of the proposed algorithm is 96.05% (Table 1); the ability of the method to produce an integrated plaque characterization map using OCT is presented in Figure 6.

Table 1: Confusion matrix of the tested patches.

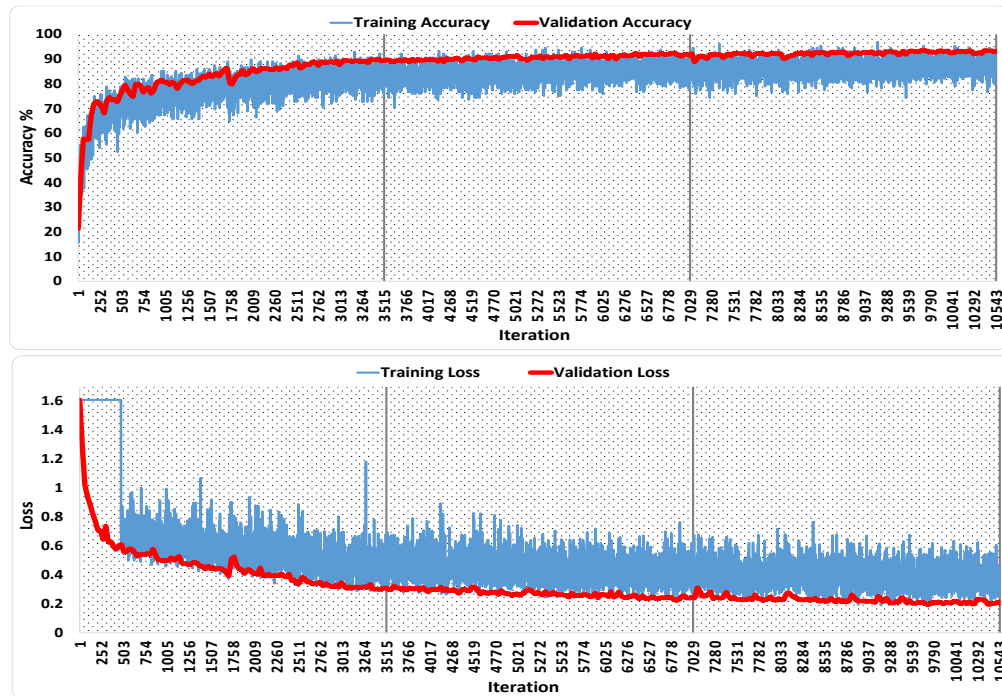| Confusion Matrix	C	LT	FT	MT	N	Accuracy
C	**6831**	959	163	1497	0	72.3 %
LT	8835	**162214**	1378	1803	218	93.0 %
FT	1451	2425	**208421**	4038	1	96.3 %
MT	1738	1782	2072	**29709**	0	84.2 %
N	1259	2629	872	168	**403315**	98.8 %
Accuracy	72.3 %	93.0 %	96.3 %	84.2 %	98.8 %	**96.05 %**

Figure 5: Training results of the CNN algorithm: Classification accuracies (top) and loss (bottom) for the training and testing data using the proposed CNN network over 3 epochs (3515 iterations each).
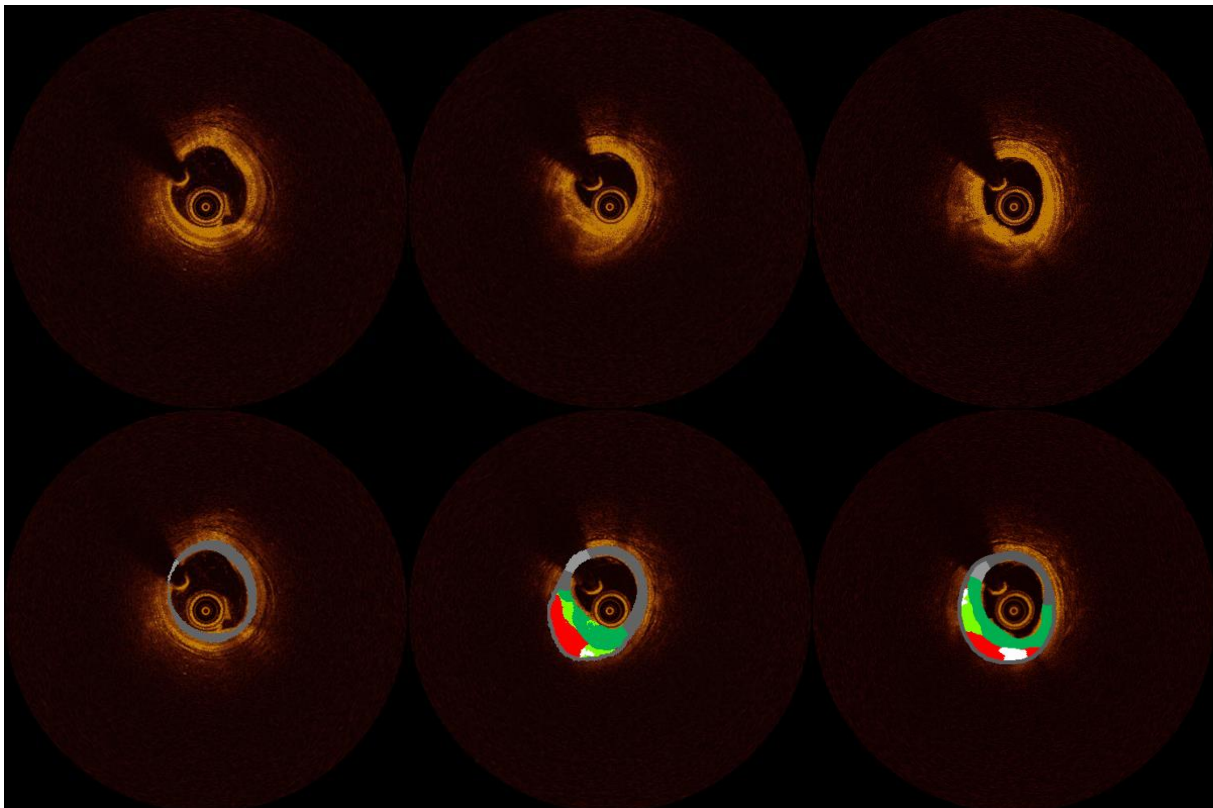

Figure 6: Application examples of the proposed integrated OCT plaque characterization method: initial images (top) and their corresponding color-coded images (bottom). C: white, LT: red, FT: green, MT: light green, N: light gray and M: dark gray.

5. DISCUSSION AND CONCLUSIONS

Few methods have been presented during the last decade for detecting and characterizing atherosclerotic plaque using OCT images[10,14–16]. These methods were primarily based on machine learning algorithms[10,13,14] and most recently on deep learning approaches using convolutional neural networks (CNN)[15,16]. These methods can sufficiently detect a large percentage of the atherosclerotic tissue within the arterial wall. However, while CNN-based methods outperformed the machine learning methods, they could not characterize the whole arterial wall as VH-IVUS[19] does.

We present an automated method that automatically detects atherosclerosis and classifies the plaque image to 5 different classes: calcium (C), lipid tissue (LT), fibrous tissue (FT), mixed tissue (MT), no visible tissue (guidewire shadow artifact; N), and detects the non-pathological tissue or media (M). The method is based on the combination of WAR detection algorithms and CNN, and was validated using the estimations of expert observers as gold standard in a large clinically-relevant dataset. Our results demonstrate reliable tissue detection and characterization, even in images having artifacts.

The method is more accurate and realistic than the methods presented previously in the literature, which makes it notably qualified for use in the clinical and research arenas. Improvements can be made as the method has lower accuracy when detecting calcific tissue (Table 1). This limitation is due to the nature of mixed tissue which includes calcium and lipid and shares image characteristics of both C and LT. Increasing the clinical dataset and incorporating histological findings in the training/testing phase of the proposed method is expected to solve the former limitation, enable its use in the clinical/research arena and enhance the field of computational cardiology[23].

6. ACKNOWLEDGMENTS

REFERENCES

[1] Vignali, L., Solinas, E. and Emanuele, E., "Research and clinical applications of optical coherence tomography in invasive cardiology: a review," Curr Cardiol Rev 10(4), 2014/06/05, 369–376 (2014).

[2] Athanasiou, L., Bruining, N., Prati, F. and Koutsouris, D., "Optical Coherence Tomography: Basic Principles of Image Acquisition," [Intravascular Imaging: Current Applications and Research Developments], IGI Global, 180–194 (2011).

[3] Bezerra, H. G., Costa, M. A., Guagliumi, G., Rollins, A. M. and Simon, D. I., "Intracoronary Optical Coherence Tomography: A Comprehensive Review Clinical and Research Applications," Jacc-Cardiovascular Interv. 2(11), 1035–1046 (2009).

[4] Tearney, G. J., Regar, E., Akasaka, T., Adriaenssens, T., Barlis, P., Bezerra, H. G., Bouma, B., Bruining, N., Cho, J., Chowdhary, S., Costa, M. A., de Silva, R., Dijkstra, J., Di Mario, C., Dudeck, D., Falk, E., Feldman, M. D., Fitzgerald, P., Garcia, H., et al., "Consensus Standards for Acquisition, Measurement, and Reporting of Intravascular Optical Coherence Tomography Studies: A Report From the International Working Group for Intravascular Optical Coherence Tomography Standardization and Validation," J. Am. Coll. Cardiol. 59(12), 1058–1072 (2012).

[5] Hou, J., Xing, L., Jia, H., Vergallo, R., Soeda, T., Minami, Y., Hu, S., Yang, S., Zhang, S., Lee, H., Yu, B. and Jang, I. K., "Comparison of Intensive Versus Moderate Lipid-Lowering Therapy on Fibrous Cap and Atheroma Volume of Coronary Lipid-Rich Plaque Using Serial Optical Coherence Tomography and Intravascular Ultrasound Imaging," Am. J. Cardiol. 117(5), 2016/01/19, 800–806 (2016).

[6] Tsantis, S., Kagadis, G. C., Katsanos, K., Karnabatidis, D., Bourantas, G. and Nikiforidis, G. C., "Automatic vessel lumen segmentation and stent strut detection in intravascular optical coherence tomography," Med Phys 39(1), 2012/01/10, 503–513 (2012).

[7] Ughi, G. J., Adriaenssens, T., Onsea, K., Kayaert, P., Dubois, C., Sinnaeve, P., Coosemans, M., Desmet, W. and D'Hooge, J., "Automatic segmentation of in-vivo intra-coronary optical coherence tomography images to assess stent strut apposition and coverage," Int J Cardiovasc Imaging 28(2), 2011/02/25, 229–241 (2012).

[8] Athanasiou, L., Rikhtegar Nezami, F., Zanotti Galon, M., Lopes, A. C., Lemos, P. A., de la Torre Hernandez, J. M., Ben-Assa, E. and Edelman, E. R., "Optimized computer-aided segmentation and 3D reconstruction using intracoronary optical coherence tomography," IEEE J. Biomed. Heal. Informatics (2018).

[9] Ahn, C. Y., Kim, B. K., Hong, M. K., Jang, Y., Heo, J., Joo, C. and Seo, J. K., "Automated Measurement of Stent Strut Coverage in Intravascular Optical Coherence Tomography," J. Korean Phys. Soc. 66(4), 558–570 (2015).

[10] Athanasiou, L. S., Bourantas, C. V., Rigas, G., Sakellarios, A. I., Exarchos, T. P., Siogkas, P. K., Ricciardi, A., Naka, K. K., Papafaklis, M. I., Michalis, L. K., Prati, F. and Fotiadis, D. I., "Methodology for fully automated segmentation and plaque characterization in intracoronary optical coherence tomography images," J. Biomed. Opt. 19(2), 026009 (2014).

[11] Olender, M. L., Athanasiou, L. S., de la Torre Hernandez, J. M., Camarero, T. G., Cascon, J. D., Consuegra-Sanchez, L. and Edelman, E. R., "Estimating the internal elastic membrane cross-sectional area of coronary arteries autonomously using optical coherence tomography images," 2017 IEEE EMBS Int. Conf. Biomed. Heal. Informatics, 109–112, IEEE (2017).

[12] Athanasiou, L. S., Fotiadis, D. I. and Michalis, L. K., [Atherosclerotic Plaque Characterization Methods Based on Coronary Imaging], Elsevier Science (2017).

[13] Xu, C. Y., Schmitt, J. M., Carlier, S. G. and Virmani, R., "Characterization of atherosclerosis plaques by measuring both backscattering and attenuation coefficients in optical coherence tomography," J. Biomed. Opt. 13(3), 34003 (2008).

[14] van Soest, G., Goderie, T., Regar, E., Koljenovic, S., van Leenders, G. L. J. H., Gonzalo, N., van Noorden, S., Okamura, T., Bouma, B. E., Tearney, G. J., Oosterhuis, J. W., Serruys, P. W. and van der Steen, A. F. W., "Atherosclerotic tissue characterization in vivo by optical coherence tomography attenuation imaging," J. Biomed. Opt. 15(1), 11105 (2010).

[15] He, S., Zheng, J., Maehara, A., Mintz, G., Tang, D., Anastasio, M. and Li, H., "Convolutional neural network based automatic plaque characterization for intracoronary optical coherence tomography images," Med. Imaging 2018 Image Process. 10574, E. D. Angelini and B. A. Landman, Eds., 107, SPIE (2018).

[16] Borges Oliveira, D. A., Nicz, P., Campos, C., Lemos, P., Macedo, M. M. G. and Gutierrez, M. A., "Coronary calcification identification in optical coherence tomography using convolutional neural networks," Med. Imaging 2018 Biomed. Appl. Mol. Struct. Funct. Imaging 10578, B. Gimi and A. Krol, Eds., 69, SPIE (2018).

[17] Kolluru, C., Prabhu, D., Gharaibeh, Y., Bezerra, H., Guagliumi, G. and Wilson, D., "Deep neural networks for A-line-based plaque classification in coronary intravascular optical coherence tomography images," J. Med. Imaging 5(04), 1 (2018).

[18] Gessert, N., Lutz, M., Heyder, M., Latus, S., Leistner, D. M., Abdelwahed, Y. S. and Schlaefer, A., "Automatic Plaque Detection in IVOCT Pullbacks Using Convolutional Neural Networks," IEEE Trans. Med. Imaging, 1–1 (2018).

[19] Konig, A. and Klauss, V., "Virtual histology," Heart 93(8), 2007/05/16, 977–982 (2007).

[20] Olender, M. L., Athanasiou, L. S., Hernandez, J. M. de la T., Ben-Assa, E., Nezami, F. R. and Edelman, E. R., "A Mechanical Approach for Smooth Surface Fitting to Delineate Vessel Walls in Optical Coherence Tomography Images," IEEE Trans. Med. Imaging, 1–1 (2018).

[21] Goodfellow, I., Bengio, Y. and Courville, A., [Deep learning].

[22] Sutskever, I., Martens, J., Dahl, G. and Hinton, G., "On the importance of initialization and momentum in deep learning," Proc. 30th Int. Conf. Mach. Learn. 28(3), S. Dasgupta and D. McAllester, Eds., 1139–1147, PMLR, Atlanta, Georgia, USA (2013).

[23] Athanasiou, L., Nezami, F. R. and Edelman, E. R., "Position Paper Computational Cardiology," IEEE J. Biomed. Heal. Informatics 23(1), 4–11 (2019).